applied sciences

Article

Influence of Small Radius Curve Shield Tunneling on Settlement of Ground Surface and Mechanical Properties of Surrounding Rock and Segment

Ping Lou [1,2,*], Yonghe Li [1], Hongbo Xiao [3], Zhengang Zhang [3] and Shide Lu [3]

[1] School of Civil Engineering, Central South University, Changsha 410075, China
[2] MOE Key Laboratory of Engineering Structures of Heavy Haul Railway, Central South University, Changsha 410075, China
[3] CCFEB Civil Engineering Co., Ltd., Changsha 410004, China
* Correspondence: pinglou@mail.csu.edu.cn; Tel.: +86-731-8265-5177; Fax: +86-731-8557-1736

Abstract: Compared with straight tunnels, over-excavation occurs on the inner side of the curved section during shield construction of small radius curved tunnels, and the disturbance to the ground surface and mechanical properties of surrounding rock and segment are more severe. This paper establishes the numerical models of small radius curve tunnels and straight tunnels to study the characteristics of surface deformation caused by the shield excavation of small radius curved tunnels and the influence of shield construction parameters on ground settlement, surrounding rock deformation, and segment force. The maximum error between the numerical simulation results and the measured surface settlement curve is 7.3%, which is in good agreement. The results show that: (1) The maximum value of the surface settlement of the small radius curve tunnel appears inside the curve section, and with the decrease in the curve radius, the surface settlement increases, and the distance between the peak settlement point and the tunnel center is larger. (2) When the curve radius of the tunnel is smaller, the lateral displacement of the ground surface moves farther to the inner side, and the range of soil mass with lateral displacement in the inner side is also wider. (3) Increasing the heading face pressure and grouting pressure can reduce surface settlement, but the heading face pressure should not exceed 350 kPa, and the grouting pressure should not exceed 250 kPa. (4) When the curve radius is smaller, the deformation of surrounding rock and the segment stress is larger.

Keywords: small radius tunnel; numerical simulation; over-excavation; ground settlement; surrounding rock deformation; segment stress

Citation: Lou, P.; Li, Y.; Xiao, H.; Zhang, Z.; Lu, S. Influence of Small Radius Curve Shield Tunneling on Settlement of Ground Surface and Mechanical Properties of Surrounding Rock and Segment. *Appl. Sci.* **2022**, *12*, 9119. https://doi.org/10.3390/app12189119

Academic Editor: Daniel Dias

Received: 10 August 2022
Accepted: 8 September 2022
Published: 11 September 2022

1. Introduction

With the rapid advancement of subway construction in the world, the technical problems faced by subway construction emerge one after another. Limited by the complex surrounding environment, it is necessary to build small radius curved tunnels to meet the line requirements of urban subways. Compared with the straight section, the over-excavation inside the curved section of the small radius curved tunnel shield construction is more obvious, and will cause greater disturbance to the ground. Therefore, it is necessary to research the influence of shield construction about small radius curve tunnels on surface deformation to ensure the stability of surface buildings.

Many scholars studied the law of ground deformation caused by tunnel shield construction. For example, Zhao et al. [1] used the compound Gauss–Legert integral to analyze the additional soil stress caused by the double-O tunnel shield construction, and corrected the maximum settlement coefficient and the width of the settlement trough coefficient about the traditional Peck formula; Zhong et al. [2] established a fine shallow-buried subway tunnel model and analyzed the influence of the main tunnel parameters on the ground settlement; Benmebarek et al. [3] used a numerical simulation to analyze the disturbance of the shallow tunnel excavation on the ground, and discussed the law of the influence of the shallow tunnel construction on the ground surface; Lou et al. [4] studied the deformation characteristics of the tunnel caused by the shield tunnel going through the foundation pit using numerical simulation and field measurement, and proposed a subsection pressure method. Koukouras et al. [5] used an artificial neural network (ANN)-based artificial intelligence system to predict ground subsidence; Wang et al. [6] combined numerical simulation with mathematical statistics, collected various monitoring data after the shield was launched, and trained the numerical model to realize real-time prediction of the development of the bottom surface settlement; Cao et al. [7] monitored the construction of the Beijing subway, and the results show that the surface settlement was mainly caused by shield excavation, slope excavation, and double arch excavation, and grouting can effectively control surface settlement; Cheng et al. [8] monitored the settlement of a large-diameter tunnel in Beijing, and observed a narrow settlement trough in the large tunnel; Fang et al. [9] conducted a tunnel excavation model test in sandy soil to study the influence of tunnel depth and ground volume loss on the longitudinal surface settlement caused by tunnel construction. Shao et al. [10] took the actual shield engineering as the research object, and studied the influence of grouting parameters on the surface settlement. You et al. [11] studied the law of surface deformation under the excavation of large-diameter shield tunnels by combining numerical simulation and field measurement. Ling et al. [12] analyzed the influence of driving pressure on surface subsidence with a finite element model, and developed a method for predicting surface subsidence. An et al. [13] studied the effect of grouting pressure on surface subsidence through numerical simulation. Qi et al. [14] studied the law of surface subsidence caused by the tunneling of overlapping double shield tunnels with a small turning radius through theoretical analysis and related experiments. Xu et al. [15] combined theory and experiment to analyze the characteristics of surface subsidence caused by small radius tunnels, and studied the influence of curve radius and tunnel depth on surface subsidence. Qiao et al. [16] studied the influence laws of small radius curve tunnel excavation parameters based on theory and combined with field measurements. Wu et al. [17] studied the law of surface subsidence caused by the excavation of small radius curved double-line shield tunnels by finite element method. Deng et al. [18] studied the law of surface subsidence caused by curved shield tunneling based on theory. Li et al. [19] studied the characteristics of additional stress caused by curved tunneling based on Mindlin theory. Feng et al. [20] studied the influence of excavation parameters on surface subsidence under small radius curved tunnel excavation through theoretical methods and numerical simulations. Lu et al. [21] established a prediction formula for land subsidence caused by shield excavation with different radii based on numerical simulation and field data.

It can be seen that most scholars [1–13] focus on the research of straight line tunnels, and some scholars [14–21] focus on the research of surface settlement and the influence of shield parameters on surface settlement for curved tunnels. However, there are few studies on the lateral and longitudinal deformation of the surface during the excavation of curved tunnels, and very few studies on surrounding rocks and segments. Therefore, it is necessary to study the lateral and longitudinal deformation of the ground surface and the mechanical characteristics of surrounding rock and segments in the process of curved tunnel excavation.

In view of this, relying on a small radius curve tunnel in a certain section of Changsha Metro Line 6, as shown in Figure 1, this paper establishes a numerical model considering the over-excavation inside the curve section, analyzes the law of ground deformation caused by shield excavation, and discusses the law of construction parameters on ground settlement, surrounding rock deformation, and segment stress. The research results provide theoretical guidance for the construction of this project.

Figure 1. Reality view of a tunnel with a small curve radius.

2. Engineering Background

A section of the Changsha Metro Line 6 tunnel is a small radius curved tunnel. The curved tunnel structure is a double-line horizontal parallel tunnel. The average covering thickness of the arch of the small radius curved tunnel is 21.6 m, the minimum radius is 355 m, and the distance between left and right lines is 12 m. The outer diameter of the segment is 6.2 m, the inner diameter is 5.5 m, and the segment depth is 1.5 m. It is prefabricated with C50 concrete and steel bars. The shield machine adopts an earth pressure balance shield machine, equipped with a set of over-excavation knives.

The thickness of each soil layer in the stratum of the tunnel is as follows: plain fill, 7.9 m; silty clay, 4.2 m; fully weathered slate, 1.5 m; and strongly weathered slate, 39.8 m. The cross section of the tunnel with a small radius curve is shown in Figure 2.

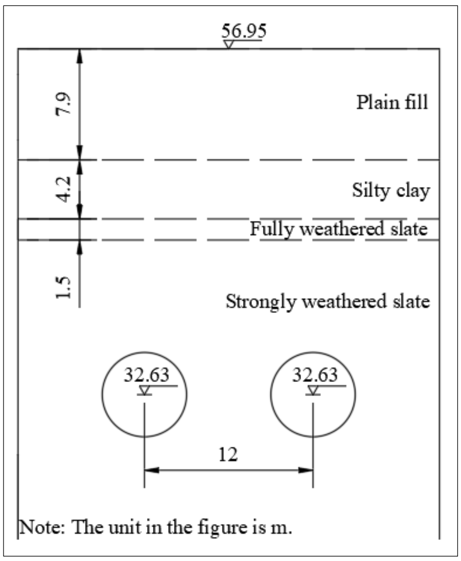

Figure 2. Schematic diagram of the cross section of the tunnel with a small radius curve.

3. Numerical Model

Midas GTS NX is a geotechnical finite element analysis software developed in Korea. It is dedicated to the finite element analysis of geotechnical and tunnel structures and is widely used in geotechnical finite element analysis, such as tunnel and foundation pit calculation. As a finite element software, Midas GTS NX cannot solve some non finite element problems, or the calculated results are not good. However, Midas GTS NX has powerful pre-processing and post-processing functions. The software interface is friendly, the interface interaction is simple and easy to understand, and the learning cycle is short.

Many researchers used and validated this software [22,23], so Midas GTS NX was used for analysis.

MIDAS GTS NX is used to establish a numerical model of a small radius curved tunnel in a certain section of the Changsha Metro Line 6. The numerical model is 60 m long along the center line of the tunnel double line, 90 m long, and 52 m high in the direction of the tunnel cross section. The schematic diagram is shown in Figure 3.

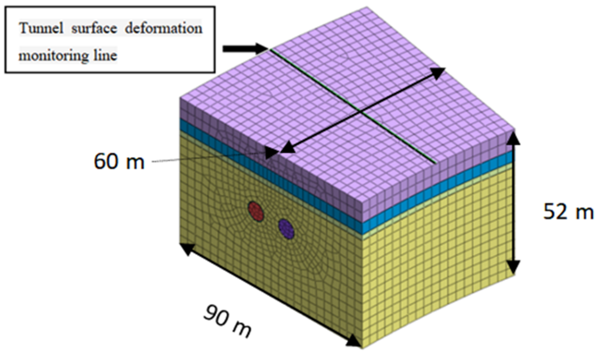

Figure 3. Numerical model of small radius curve tunnel.

In the numerical model, the outer tunnel is firstly excavated, and then the inner tunnel. The soil is simulated by a three-dimensional solid element, considering various engineering properties of the on-site soil measurement, and its constitutive model adopts the modified Mohr Coulomb model [24]. The segment and grouting layer are simulated by solid element. The shield shell is simulated by shell element. Normal and horizontal constraints are applied to the bottom of the model, normal constraints are applied to the sides of the model, and the top of the model is a free surface [25]. In order to simulate the grouting process, an equal thickness and homogeneous equivalent layer elastomer is used to simulate the grouting layer [26]. In addition, the shield machine's own weight is simulated by appropriately increasing the density of the shield machine shell. At the same time, in order to simulate the real situation near the tunnel excavation as much as possible and improve the calculation efficiency, the grid near the tunnel excavation is slightly fine, with a size of 1 m. The grid near the boundary is slightly coarse, and the size is 3 m. In the model, the slurry properties (elastic modulus) are changed to simulate the process of the slurry from soft to hard. The elastic moduli of the grouting layer during the grouting hardening process are 1 MPa and 10 MPa in the softening and hardening stages, respectively [27]. Table 1 shows the physical parameters of each material in the numerical model.

Table 1. Physical parameters of each material.

Different Soil (Rock) and Materials	Bulk Density (kN/m^3)	Cohesion (kN/m^2)	Friction Angle (°)	Elastic Modulus (kN/m^2)	Poisson's Ratio
plain fill	19	16	10	4000	0.286
silty clay	19	15	8	6000	0.31
fully weathered slate	20	35	15	8500	0.231
strongly weathered slate	23.3	50	29	120,000	0.2
segment	25	-	-	3.45 × 107	0.2
grout	22	-	-	1000 (soft) 10,000 (hard)	0.2
Shield shell	78.5	—	—	210,000,000	0.2

The construction load of the shield tunnel is as follows: the grouting pressure is 200 kPa, which is applied to the segment and the surrounding rock, respectively, the driving pressure is 250 kPa, which is applied to the driving surface, and the jack force is 200 kPa, which acts on the section of the segment. It should be mentioned that the value of each parameter remains unchanged if there is no declaration.

Unlike straight tunnel shield excavation, curved tunnel excavation requires the use of an over-excavating knife to over-excavate the inner side of the curved section to help the shield machine turn. Figure 4 is a schematic diagram of the over-excavation part of the ground loss.

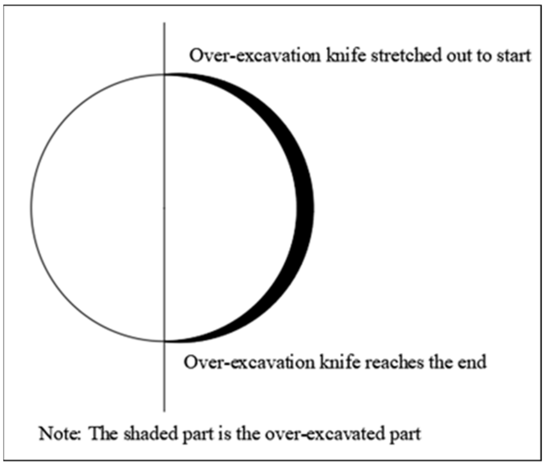

Figure 4. Schematic diagram of the formation loss of the over-excavated part on the inner side of the curve.

According to the research of the scholar [28] on the over-excavation amount on the inner side of the curve tunnel shield construction line, it can be seen that the over-excavation amount δ on the inner side of the curve section is as follows:

$$\delta = \frac{\sqrt{(2R+D)^2 + L^2} - (2R+D)}{2} \quad (1)$$

where R is the curve radius, which is 355 m in this paper, D is the shield shell diameter, which is 6.6 m, and L is the single-ended shield shell length, which is 10 m. In this project, δ is calculated to be 36.95 mm.

In the numerical model, the stratum loss section is corrected to make it more in line with the real situation of stratum loss caused by shield tunnel excavation in the curve section.

4. Model Validation

In order to verify the reliability of the numerical model built in this paper, corresponding monitoring points are set up to monitor the surface subsidence in the process of shield tunneling. Seven monitoring points are arranged in the middle section of this area, and the layout of the monitoring points is shown in Figure 5. The surface subsidence of this section is measured and data are collected by a Trimble DiNi03 leveling instrument, and the monitoring frequency is one time for each day. In this paper, the average value of the measured data of each monitoring point during the monitoring week is selected as the verification model data. After the shield construction is completed, the measured results and numerical simulation results of the surface settlement are shown in Figure 6, and the error calculation of the cross section monitoring data and the numerical simulation results are shown in Table 2.

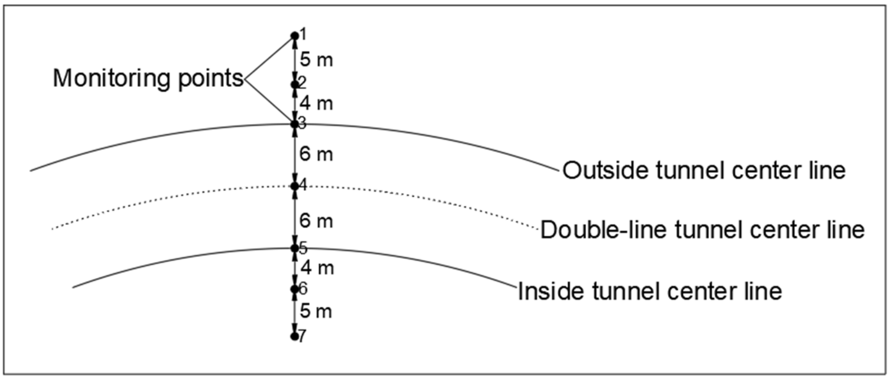

Figure 5. Layout of monitoring points.

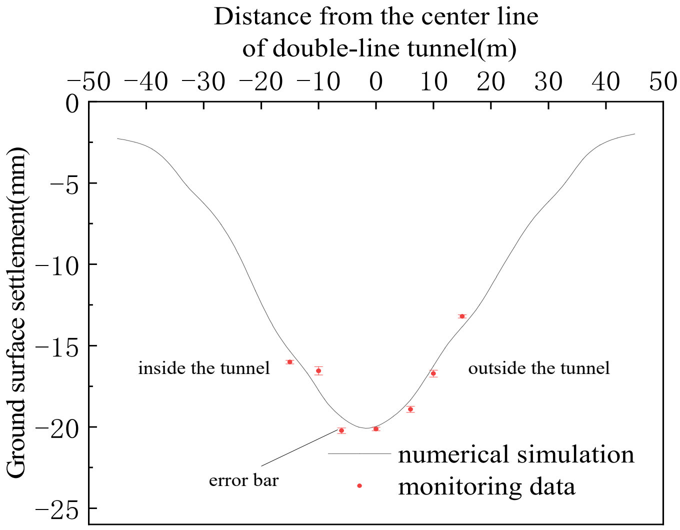

Figure 6. Comparison of measured surface settlement and numerical simulation results.

Table 2. Comparison of measured and numerical simulation results at three sections.

Monitoring Points	Numerical Simulation (mm)	Measured Data/Standard Deviation (mm)	Relative Error
1	−13.84	−13.20/0.10	4.9%
2	−16.25	−16.72/0.21	2.8%
3	−18.34	−18.92/0.19	3.1%
4	−19.98	−20.13/0.11	0.8%
5	−19.40	−20.23/0.17	4.1%
6	−17.76	−16.55/0.26	7.3%
7	−15.34	−16.01/0.11	4.2%

It can be seen from Figure 6 that the settlement trends of the ground surface are similar for the numerical simulation results and the measured results, the position of the maximum value of surface settlement is relatively close, and the shape of the surface settlement curve is relatively close. It can be seen from Table 2 that the measured data at each section monitoring point have a certain deviation. This is due to the measurement error of the instrument and the incomplete settlement of the ground surface, but its deviation is small, and the maximum standard deviation is 0.26 mm. The measured data can meet the accuracy requirements. However, the maximum error between the numerical simulation and the measured results is 7.3%, and the results of the two are relatively consistent, which verifies the accuracy of the numerical simulation results and the rationality of the recommended values of the shield construction parameters in this paper to a certain extent.

5. Numerical Simulation Results

5.1. The Settlement Analysis of Ground Surface

In order to explore the influence of different curve radii on the surface subsidence, this paper selects four types of shield tunnels as the research objects, namely 100 m, 350 m, 600 m, and straight tunnels, and selects the line between the inner and outer centers of the surface of the curve model in Figure 3 as the monitoring line and records the surface settlement value. The surface settlement curves of different tunnels are shown in Figure 7.

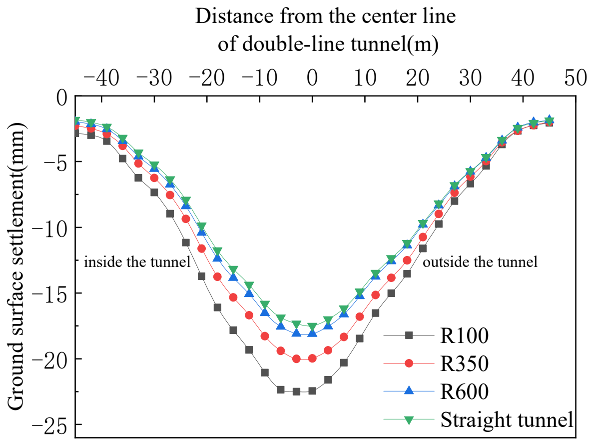

Figure 7. Settlement curve of surface soil after double-track tunnel excavation.

It can be seen from Figure 7 that the settlement curves of the four types of tunnels are basically the same, and a V-shaped settlement tank is formed on the ground surface, but the settlement of the curved tunnel is not uniform, and the peak settlement appears inside the tunnel centerline, which is mainly due to the process of the curved shield tunnel excavation. It is caused by factors such as over-excavation in the middle and inner side and uneven force. The maximum settlement of a curve radius with 100 m, 350 m, 600 m, and the straight tunnel is 22.50 mm, 20.01 mm, 18.10 mm, and 17.50 mm, respectively. It can be seen that the maximum surface settlement increases with the decrease in the curve radius, which is consistent with the reference [15]. Compared with the straight tunnel, the maximum surface settlement of the three curved tunnels increased by 28.57%, 14.34%, and 3.44%, respectively. At the same time, it can also be found that with the decrease in the curve radius, the distance between the peak settlement point and the tunnel center continues to increase. Similar conclusions can be found in the reference [21]. It can be seen that the over-excavation of the inner side of the curve section by the shield construction of the small radius curve tunnel will aggravate the surface settlement and change the position of the maximum surface settlement.

5.2. The Lateral Displacement Analysis of Ground Surface

In order to study the difference between the lateral displacement characteristics of the curved tunnel and the straight tunnel, a curved tunnel with a curved radius of 350 m and a straight tunnel were established, respectively, and the influence of the curved radius on the lateral displacement of the ground surface was studied. The lateral displacement of the surface soil after the excavation of the small radius curve and the straight tunnel is shown in Figure 8.

It can be seen from Figure 8 that the lateral displacement of the soil on both sides of the conventional straight tunnel after shield excavation is roughly symmetrically distributed with the double-line center line of the tunnel as the axis, which is consistent with the research conclusions of some scholars [29,30]. The lateral displacement of the soil on both sides of the tunnel with a small radius curve after shield excavation shows an obvious asymmetric shape with the double-line center line of the tunnel as the axis, and the lateral displacement of the soil on the inner side of the curve section is wider.

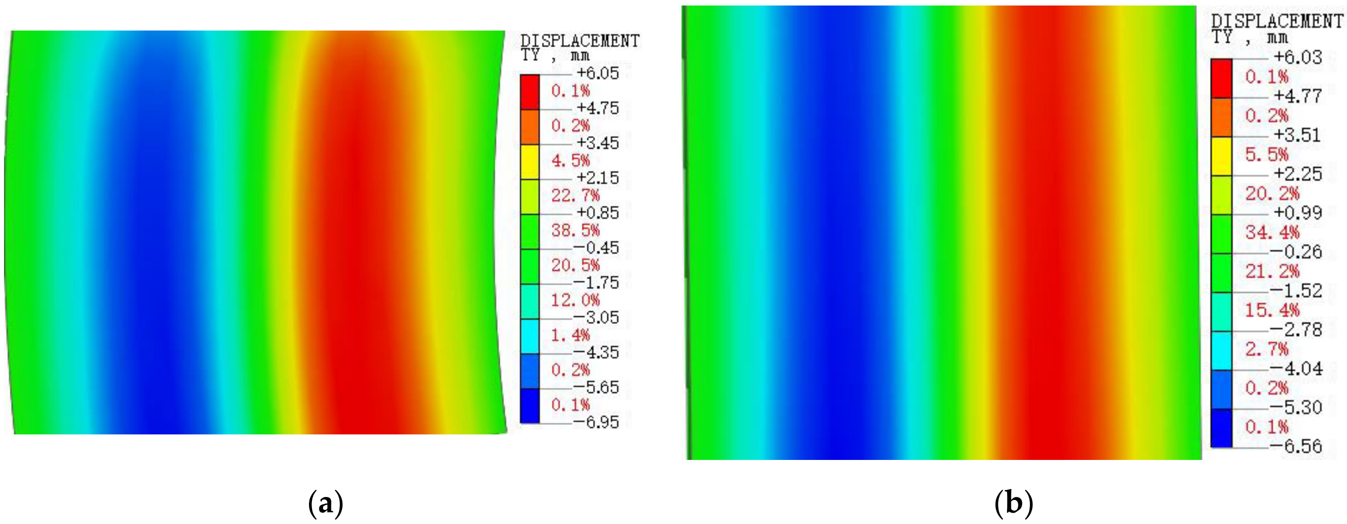

Figure 8. Lateral displacement of surface soil after double-track tunnel excavation: (**a**) lateral displacement of surface soil in small radius curve tunnel; (**b**) lateral displacement of surface soil in straight tunnel.

At the same time, in order to explore the influence of different curve radii on the lateral displacement of the ground, this paper selects four types of shield tunnels as the research objects, namely 100 m, 350 m, 600 m, and straight tunnels, and selects the line between the inner and outer centers of the surface of the curve model in Figure 2 as the monitoring line, and records the lateral displacement value of the surface here. The lateral displacement value of the ground surface at different tunnels is shown in Figure 9.

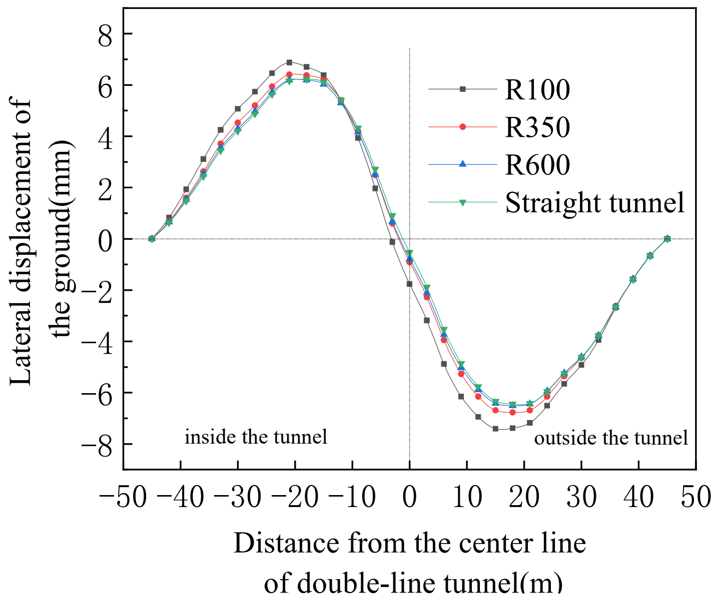

Figure 9. Lateral surface displacement curve after double-track excavation of a small radius curved tunnel.

It can be seen from Figure 9 that the lateral displacement curves of the ground surface after the excavation of tunnels with different curve radii are basically the same, that is, the lateral displacement of the ground surface on the outside of the curve section changes more obviously. The maximum lateral displacement of the curve radius with 100 m, 350 m, 600 m, and the straight tunnel is 7.40 mm, 6.77 mm, 6.50 mm, and 6.45 mm, respectively. Taking the lateral displacement corresponding to the straight tunnel as the benchmark, the lateral displacement of the surface corresponding to the curve radius of 100 m, 350 m, and 600 m increased by 14.85%, 4.98%, and 0.88%, respectively. This is because when the radius of the curve is smaller, the more the stratum is over-excavated inside the curve section, the more intensified the stratum disturbance. It can also be found that the lateral displacement of the surface of the tunnel with the curve radius will move inward, and the soil body with lateral displacement on the inside is wider. The lateral displacement of the soil will cause a shear layer in the stratum and affect the structural stability of the shallow foundation building. Therefore, it is necessary to consider the reinforcement of the building on the inner side of the curve before the shield construction of the small radius curve tunnel.

5.3. The Longitudinal Displacement Analysis of Ground Surface

Taking small curved tunnels with a curve radius of 350 m and straight tunnels as the research object, and taking the surface settlement state of the tunnel double-line center line when the shield machine cutter head is advanced 40 m for analysis, the curve of the small radius curve and the linear tunnel double-line center line of the surface settlement, as well as the distance from the shield machine, are shown in Figure 10.

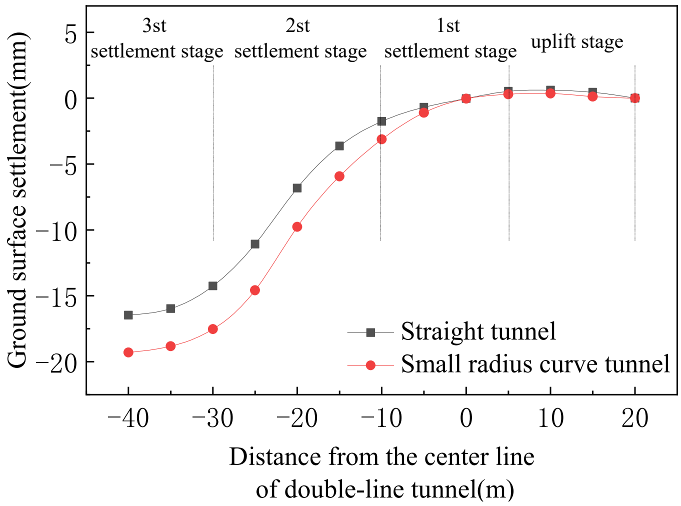

Figure 10. Variation curve of ground settlement and distance from the shield machine.

It can be seen from Figure 10 that during the shield excavation of the small radius curve and straight tunnel, the surface in front of the shield machine cutter head slightly uplifts, and the ground surface behind the shield machine begins to settle sharply after excavation, and finally the surface settlement slows down. This is similar to the results in reference [20].

The curve of the surface settlement of the tunnel with a small radius curve and the distance from the shield machine shows that the surface of the shield machine has a slight subsidence from 0 m to 9 m behind the cutter head of the shield machine. In the soil layer below the surface, only a small amount of subsidence occurs on the surface. The surface subsidence of 9 m to 24 m behind the cutter head of the shield machine develops the fastest. At this time, the soil layer below the surface is supported by pipe segments and grouting. The formation loss and the softening of the grout make the surface subsidence sharply expand. The surface subsidence at this stage accounts for 53.17% of the total subsidence. After 24 m behind the cutter head of the shield machine, the surface settlement rate slows down. At this time, the grout gradually hardens to support the surrounding soil, and soil consolidation becomes the dominant factor for surface settlement at this time.

Through the above analysis, it can be found that the ground settlement caused by shield excavation can be roughly divided into three stages: in the first stage, the ground settlement is caused by ground disturbance when the shield machine passes through; in the second stage, segment assembly and slurry softening of the ground settlement is caused by formation loss; and in the third stage, the ground subsidence is caused by the consolidation of the soil after the shield machine passes.

It can be seen from Figure 9 that the second stage is the main reason for the difference in surface settlement between the straight line and small radius curved tunnels. Due to the greater stratum loss during the excavation of the small radius curve tunnel, the surface settlement develops faster in the second stage. In view of the development characteristics of the surface settlement in the second stage, accelerating the grouting speed and reducing the time of grout hardening are effective ways to reduce surface settlement.

6. Influence Analysis of Shield Tunneling Parameters

6.1. Influence of Heading Face Pressure on Ground Settlement

In the numerical model of the small radius curve tunnel, in order to explore the influence of the heading face pressure on the surface settlement, the heading face pressure is taken as 180 kPa, 240 kPa, 300 kPa, 360 kPa, 420 kPa, 480 kPa, and 540 kPa for numerical simulation. The curve of surface settlement with the pressure of the heading face is shown in Figure 11.

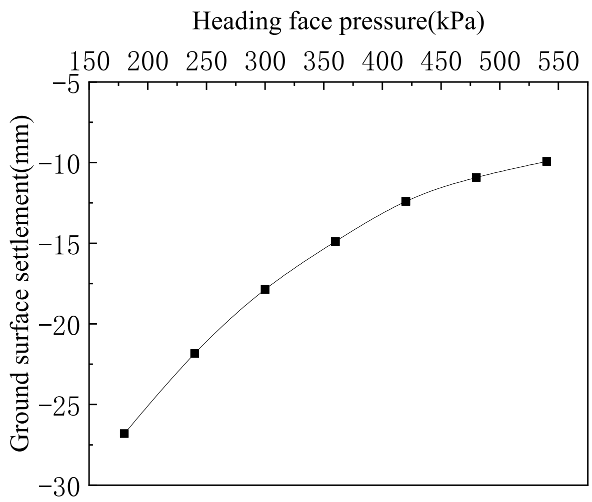

Figure 11. Curve of surface settlement with the pressure of the heading face.

It can be seen from Figure 11 that when the heading face pressure of the shield machine is 180 kPa, the surface settlement value is 26.8 mm. As the heading face pressure of the shield machine gradually increases, the surface settlement value gradually decreases. Taking the surface settlement when the heading face pressure is 180 kPa as the benchmark, the surface settlement decreases by 18.52%, 33.33%, 44.43%, 53.70%, 59.26%, and 62.96% for every 60 kPa increase in the heading surface pressure.

When the heading face pressure is 300~350 kPa, the surface settlement control effect is better. If the heading face pressure is further increased, on the one hand, it will have little effect on improving the surface settlement. On the other hand, the large heading face pressure means that the high energy consumption of the shield machine is not conducive to the cost control of the enterprise.

Considering the background of the small radius curved tunnel of Changsha Metro Line 6, the pressure of the heading face is recommended to be 300~350 kPa.

6.2. The Influence of Grouting Pressure on Surface Settlement

The larger grouting pressure squeezes the segment and surrounding rock, which may lead to segment fracture and surrounding rock splitting. The smaller grouting pressure makes it difficult to restrain the deformation of surrounding rock, resulting in the larger settlement of ground surface, especially when the tunnel is located in a curved section; not only is the force on the inside and outside of the curve uneven, but also the inside of the tunnel needs to be over-excavated, causing greater soil disturbance. Therefore, it is necessary to further study the effect of grouting pressure on surface settlement, surrounding rock deformation, and segment stress.

6.2.1. Influence of Grouting Pressure on Surface Settlement

In order to explore the influence of the grouting pressure on the surface settlement, the grouting pressure is, respectively, taken as 50 kPa, 100 kPa, 150 kPa, 200 kPa, 300 kPa, 400 kPa, and 500 kPa. The change curve of surface settlement with synchronous grouting pressure is shown in Figure 12.

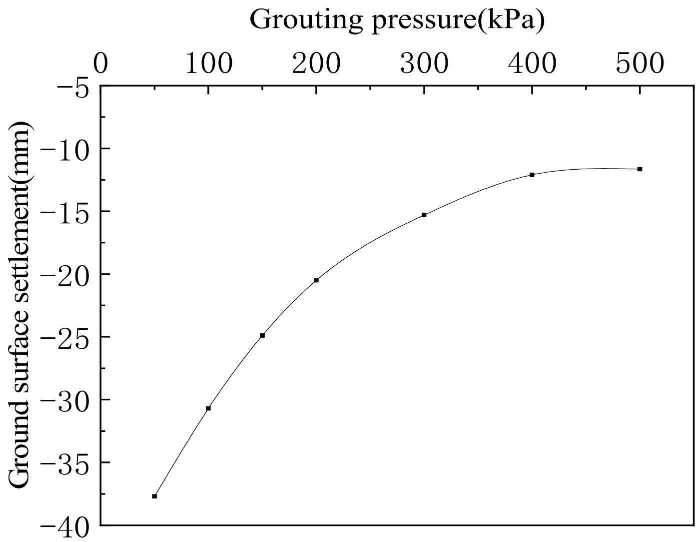

Figure 12. Curve of surface settlement with simultaneous grouting pressure.

It can be seen from Figure 12 that when the synchronous grouting pressure of the shield machine is 50 kPa, the surface settlement value is 37.7 mm. As the synchronous grouting pressure of the shield machine gradually increases, the surface settlement value gradually decreases. The reason for this is that the smaller grouting pressure makes it difficult to balance the surrounding rock pressure, resulting in a large deformation of the surrounding rock, and similar laws can be found in reference [31]. Taking the surface settlement when the grouting pressure is 50 kPa as the benchmark, the surface settlement decreases by 18.57%, 33.95%, 46.42%, 51.99%, 59.42%, 64.46%, and 67.90% for every 50 kPa increase in grouting pressure.

When the grouting pressure is 250 kPa, the surface settlement control effect is better. If the grouting pressure is further increased, on the one hand it will not have much effect on improving the surface settlement, but on the other hand, it may affect the force of the segment. The stress form of the tunnel segments with small radius curves is more complicated, and whether it can withstand the large grouting pressure remains to be discussed.

6.2.2. Influence of Grouting Pressure on Mechanical Properties of Surrounding Rock

Tunnel excavation causes the redistribution of surrounding rock stress, resulting in the reduction in the surrounding rock strength and even damage [21], in particular, the profile of the excavation surface formed by the small curve shield tunnel is different, which leads to uneven stress on the surrounding rock, which may lead to the instability of the surrounding rock. In this paper, the shear stress and shear strain of the surrounding rock are taken as the evaluation indexes, the grouting pressure is, respectively, taken as 50 kPa, 100 kPa, 150 kPa, 200 kPa, 300 kPa, 400 kPa, and 500 kPa. The relationship curves of the maximum shear stress of the surrounding rock, the maximum shear strain of the surrounding rock, and the grouting pressure obtained by calculation are shown in Figures 13 and 14, respectively.

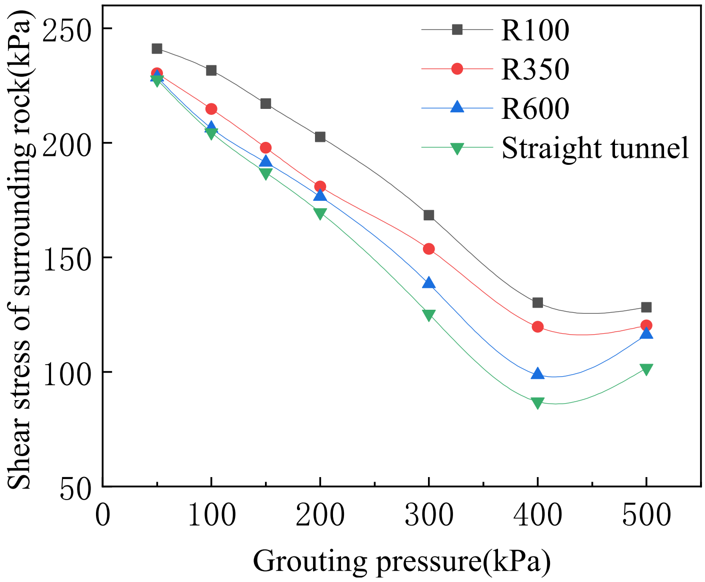

Figure 13. Variation curve of maximum shear stress of surrounding rock with the grouting pressure.

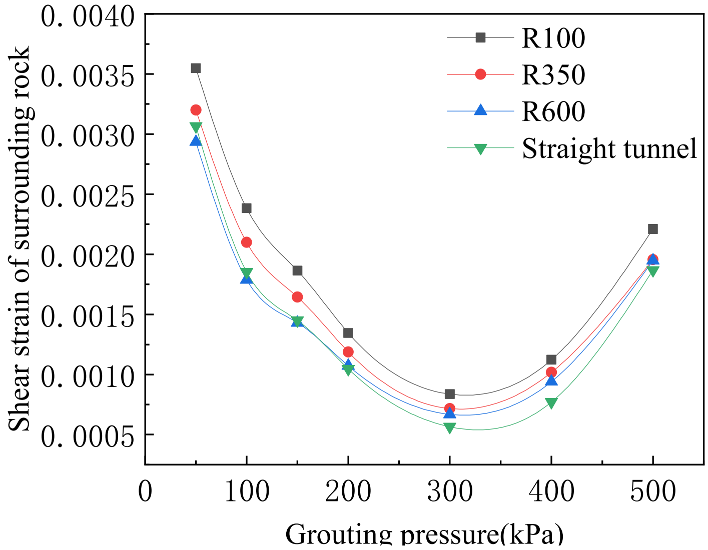

Figure 14. Variation curve of maximum shear strain of surrounding rock with the grouting pressure.

It can be seen from Figure 13 that the variation trend of the maximum shear stress of the surrounding rock with the grouting pressure of the four tunnels is similar, that is, when the grouting pressure is less than 400 kPa, the maximum shear stress of the surrounding rock decreases, and when it is greater than 400 kPa, the maximum shear stress of the surrounding rock decreases. Then, it increases slowly, because the larger grouting pressure squeezes the surrounding rock or even destroys the surrounding rock. When the grouting pressure is 200 kPa, and the maximum shear stress of the surrounding rock with a curve radius of 100 m, 350 m, 600 m, and the straight tunnel is 202.6 kPa, 180.9 kPa, 176.6 kPa, and 169.6 kPa, respectively. Compared with the maximum shear stress of the surrounding rock with the straight tunnel, the maximum shear stress of the surrounding rock corresponding to the curve radius of 100 m, 350 m, and 600 m increased by 19.46%, 6.66%, and 4.13%, respectively. This is because the smaller the curve radius is, the more uneven the force on the surrounding rock is, which leads to greater stress on the surrounding rock. It can be seen that under the same conditions, the smaller the curve radius is, the easier the surrounding rock is to be unstable and damaged.

It can be seen from Figure 14 that when the grouting pressure is less than 300 kPa, the maximum shear strain of the surrounding rock decreases with the increase in the grouting pressure. When it exceeds 300 kPa, the maximum shear strain of the surrounding rock increases rapidly with the grouting pressure. The reason is that when the grouting pressure is too large, the surrounding rock is squeezed excessively, and the surrounding rock will be split and large deformation will occur. At the same time, it can be found that when the grouting pressure is constant, the smaller the curve radius of the shield tunnel is, the greater the maximum shear strain of the surrounding rock is, and the easier the failure occurs. When the grouting pressure is 200 kPa, compared with the straight tunnels, the maximum surrounding rock shear strain of the three curved tunnels increases by 28.43%, 13.47%, and 2.42%, respectively. It can be seen that the tunnel radius and grouting pressure have a great influence on the stability of the surrounding rock.

It can be seen that the grouting pressure and the radius of the tunnel curve have a certain influence on the stability of the surrounding rock. A moderate increase in the grouting pressure is helpful to improve the stability of the surrounding rock. When the grouting pressure is constant, the smaller the radius of the curve is, the greater the maximum shear stress of the surrounding rock and the maximum shear strain of the surrounding rock will be, and the more easily unstable the surrounding rock will be. Therefore, in the actual construction process, it is necessary to adjust the posture of the shield, increase the radius of the shield tunnel curve as much as possible, and improve the stability of surrounding rock.

6.2.3. Influence of Grouting Pressure on Mechanical Properties of Segment

During the excavation process of the shield tunnel with the small curve radius, due to the uneven force on the inside and outside of the tunnel and the over-excavation on the inside, the force on the segment may be further increased. The grouting pressures were taken as 50 kPa, 100 kPa, 150 kPa, 200 kPa, 300 kPa, 400 kPa, and 500 kPa, respectively. The variation curves of the maximum longitudinal tensile stress and the maximum circumferential stress of the segment with grouting pressure are shown in Figures 15 and 16.

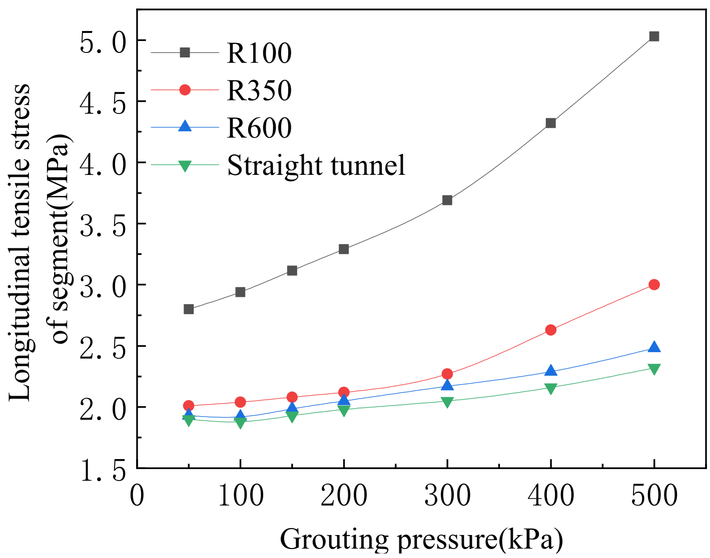

Figure 15. Variation curve of the maximum longitudinal tensile stress of the segment with the grouting pressure.

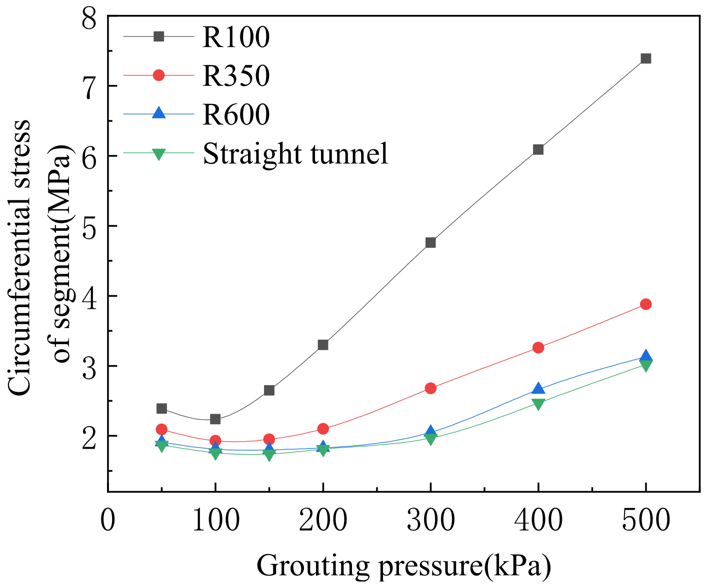

Figure 16. Variation curve of the maximum circumferential stress of the segment with the grouting pressure.

It can be seen from Figure 15 that the grouting pressure has a great influence on the longitudinal tensile stress of the segment when the tunnel is excavated. The longitudinal tensile stress of the segment increases with the increase in the grouting pressure, and the two have an obvious nonlinear relationship. When the grouting pressure is constant, the maximum longitudinal tensile stress of the segment increases with the decrease in the curve radius; especially when the tunnel radius is 100 m, the longitudinal tensile stress of the segment increases rapidly. When the grouting pressure is 200 kPa, the maximum longitudinal tensile stress with a curve radius of 100 m, 350 m, 600 m, and the straight tunnel is 3.29 MPa, 2.12 MPa, 2.05 MPa, and 1.98 MPa, respectively. The longitudinal tensile stress of the segment corresponding to the curve radius of 100 m, 350 m, and 600 m increased by 66.16%, 7.07%, and 3.54%, respectively. The reason is that when the curve radius is smaller, the jack force in the shield tunneling process is not related to the segment. The larger the direction angle is, the more the uneven force on the segment will cause additional stress on the segment.

Figure 16 also shows that the maximum circumferential stress of the four tunnel segments increases with the increase in grouting pressure. When the curve radius is 100 m, the circumferential stress changes more obviously, and the circumferential stress of the segment increases with the curve radius. When the grouting pressure is 200 kPa, the maximum longitudinal tensile stress with curve radius of 100 m, 350 m, 600 m, and the straight tunnel is 3.30 MPa, 2.10 MPa, 1.83 MPa, and 1.81 MPa, respectively. Compared with the longitudinal tensile stress of the segment of the tunnel, the longitudinal tensile stress of the segment corresponding to the curve radius of 100 m, 350 m, and 600 m increased by 82.32%, 16.02%, and 1.10%, respectively. It can be seen that the curve radius of the shield tunnel has a certain influence on the force of the segment.

To sum up, it can be seen that appropriately increasing the grouting pressure helps to control the surface subsidence, the deformation of the surrounding rock, and the stress of the segment, and the radius of the curve also has a certain influence on the three. Therefore, the radius of the tunnel should be increased as much as possible in the design stage. In this project, it is recommended that the grouting pressure be 200–250 kPa.

In cities with dense engineering buildings, limited by the complex surrounding environment, it is necessary to build small radius curved tunnels to meet the line requirements of urban subway. The over break in the arc section of small radius arc tunnel shield construction is more obvious, and not only causes greater disturbance to the ground, but also has a greater impact on the stability of the surrounding rock and the stress of segments in zone II. According to the research results, a smaller curve radius will cause greater soil deformation and segment stress. It is suggested that engineers and designers should not only consider the surface deformation, but also pay attention to the mechanical characteristics of surrounding rock and segments.

However, this paper also has some limitations. It mainly focuses on the discovery of interaction laws, only discusses the influence of grouting pressure on excavation pressure, and does not study the influence laws of tunnel parameters, such as shield tail clearance. At the same time, the equivalent layer is used to simulate the grouting layer. The relevant parameters were not obtained experimentally, which will lead to certain errors. In the future, we will continue to promote this work, comprehensively explore the influence law of shield parameters, obtain relevant parameters in combination with experiments, and further explore methods and technologies to ensure safe tunneling of shield tunnels under special conditions.

7. Conclusions

Taking the small radius curve tunnel of a certain section of Changsha Metro Line 6 as the engineering background, this paper establishes a numerical model of a small radius curve and straight tunnel, analyzes the law of surface deformation caused by the shield excavation of the small radius curve and straight tunnel, and studies the construction parameters influence on surface settlement, surrounding rock deformation, and segment stress. The research conclusions are as follows:

(1) Compared with straight tunnels, shield excavation of small radius curved tunnels will aggravate the surface settlement, and the maximum surface settlement will appear on the inner side of the curve section, and as the radius of the curve decreases, the surface subsidence increases, and the distance between the peak subsidence point and the center of the tunnel increases.
(2) When the curve radius of the tunnel is smaller, the lateral displacement of the ground surface moves farther to the inner side, and the range of soil mass with lateral displacement in the inner side is wider.
(3) Increasing the heading face pressure and grouting pressure can reduce surface settlement, but the heading face pressure should not exceed 350 kPa, and the grouting pressure should not exceed 250 kPa.
(4) When the curve radius is smaller, the deformation of the surrounding rock and the segment stress are larger.

Author Contributions: Conceptualization, methodology, supervision, review and editing, P.L.; software, validation and original draft preparation, Y.L.; resources, funding acquisition, H.X., Z.Z. and S.L. All authors have read and agreed to the published version of the manuscript.

Funding: This work was supported by the Key Project of Science and Technology Plan in Yuhua District, Changsha City (YHKJ2019-ZG-02).

Institutional Review Board Statement: Not applicable.

Informed Consent Statement: Not applicable.

Conflicts of Interest: The authors declare no conflict of interest.

References

1. Zhao, W.; Jia, P.J.; Zhu, L.; Cheng, C.; Han, J.Y.; Chen, Y.; Wang, Z.G. Analysis of the additional stress and ground settlement induced by the construction of double-o-tube shield tunnels in sandy soils. *Appl. Sci.* **2019**, *9*, 2246–2251. [CrossRef]
2. Zhong, Z.L.; Li, C.; Liu, X.R.; Fan, Y.F.; Liang, N.H. Analysis of ground surface settlement induced by the construction of mechanized twin tunnels in soil-rock mass mixed ground. *Tunn. Undergr. Space Technol.* **2021**, *83*, 520–532. [CrossRef]
3. Benmebarek, S.; Kastner, R. Numerical modeling of ground movements caused by tunneling. *Can. Geotech. J.* **2000**, *37*, 1309–1324. [CrossRef]
4. Lou, P.; Li, Y.H.; Lu, S.D.; Xiao, H.B.; Zhang, Z.A. Deformation and mechanical characteristics of existing foundation pit and tunnel itself caused by shield tunnel undercrossing. *Symmetry* **2022**, *14*, 263. [CrossRef]

5. Koukoutas, S.P.; Sofianos, A.I. Settlements due to Single and Twin Tube Urban EPB Shield tunnelling. *Geotech. Geol. Eng.* **2015**, *33*, 487–510. [CrossRef]
6. Wang, F.; Gou, B.C.; Zhang, Q.L.; Qin, Y.W.; Li, B. Evaluation of ground settlement in response to shield penetration using numerical and statistical methods: A metro tunnel construction case. *Struct. Infrastruct. Eng.* **2016**, *12*, 1024–1037. [CrossRef]
7. Cao, L.Q.; Fang, Q.; Zhang, D.L.; Chen, T.L. Subway station construction using combined shield and shallow tunnelling method: Case study of Gaojiayuan station in Beijing. *Tunn. Undergr. Space Technol.* **2018**, *82*, 627–635. [CrossRef]
8. Cheng, H.Z.; Chen, J.; Chen, G.L. Analysis of ground surface settlement induced by a large EPB shield tunnelling: A case study in Beijing, China. *Environ. Earth Sci.* **2019**, *78*, 605. [CrossRef]
9. Fang, Y.; Chen, Z.T.; Tao, L.M.; Cui, J.; Yan, Q.X. Model tests on longitudinal surface settlement caused by shield tunnelling in sandy soil. *Sust. Cities Soc.* **2019**, *47*, 101504. [CrossRef]
10. Shao, X.K.; Yang, Z.Y.; Jiang, Y.S.; Yang, X.; Qi, W.Q. Field test and numerical study of the effect of shield tail-grouting parameters on surface settlement. *Geomech. Eng.* **2022**, *29*, 509–522.
11. You, S.; Sun, J.A. Deformation and control of super-large-diameter shield in the upper-soft and lower-hard ground crossing the embankment. *Appl. Sci.* **2022**, *12*, 4324. [CrossRef]
12. Ling, X.Z.; Kong, X.X.; Tang, L.; Zhao, Y.Z.; Tang, W.C.; Zhang, Y.F. Predicting earth pressure balance (EPB) shield tunneling-induced ground settlement in compound strata using random forest. *Transp. Geotech.* **2022**, *35*, 100771. [CrossRef]
13. An, J.B.; Kang, S.J.; Cho, G.C. Numerical evaluation of surface settlement induced by ground loss from the face and annular gap of EPB shield tunneling. *Geomech. Eng.* **2022**, *29*, 291–300.
14. Qi, W.Q.; Yang, Z.Y.; Jiang, Y.S.; Yang, X.; Shao, X.K.; An, H.B. Investigation on ground displacements induced by excavation of overlapping twin shield tunnels. *Geomech. Eng.* **2022**, *28*, 531–546.
15. Xu, P.; Xi, D.H. Investigation on the surface settlement of curved shield construction in sandy stratum with laboratory model test. *Geotech. Geol. Eng.* **2021**, *39*, 5493–5504. [CrossRef]
16. Qiao, S.F.; Xu, P.; Liu, R.T.; Wang, G. Study on the horizontal axis deviation of a small radius TBM tunnel based on Winkler foundation model. *Appl. Sci.* **2020**, *10*, 784. [CrossRef]
17. Wu, D.Z.; Xu, K.P.; Guo, P.P.; Lei, G.; Cheng, K.; Gong, X.N. Ground deformation characteristics induced by mechanized shield twin tunnelling along curved alignments. *Adv. Civ. Eng.* **2021**, *2021*, 6640072. [CrossRef]
18. Deng, H.S.; Fu, H.L.; Yue, S.; Huang, Z.; Zhao, Y.Y. Ground loss model for analyzing shield tunneling-induced surface settlement along curve sections. *Tunn. Undergr. Space Technol.* **2022**, *119*, 104250. [CrossRef]
19. Li, S.S.; Li, P.F.; Zhang, M.J. Analysis of additional stress for a curved shield tunnel. *Tunn. Undergr. Space Technol.* **2021**, *107*, 103675. [CrossRef]
20. Feng, X.J.; Wang, P.; Liu, S.F.; Wei, H.; Miao, Y.L.; Bu, S.J. Mechanism and law analysis on ground settlement caused by shield excavation of small-radius curved tunnel. *Rock Mech. Rock Eng.* **2022**, *55*, 3473–3488. [CrossRef]
21. Lu, L.H.; Sun, J.C.; Zhou, G.F.; Tan, S.Y.; Liu, H.; Li, G. Research on the surface deformation prediction for curved shield construction in clay stratum. *J. Railw. Eng. Soc.* **2018**, *35*, 99–105. (In Chinese)
22. Alagha, A.S.N.; Chapman, D.N. Numerical modelling of tunnel face stability in homogeneous and layered soft ground. *Tunn. Undergr. Space Technol.* **2019**, *94*, 10. [CrossRef]
23. Alzabeebee, S.; Chapman, D.N.; Faramarzi, A. Development of a novel model to estimate bedding factors to ensure the economic and robust design of rigid pipes under soil loads. *Tunn. Undergr. Space Technol.* **2018**, *71*, 567–578. [CrossRef]
24. Xie, S.J.; Lin, H.; Chen, Y.F.; Wang, Y.X. A new nonlinear empirical strength criterion for rocks under conventional triaxial compression. *J. Cent. South Univ.* **2021**, *28*, 1448–1458. [CrossRef]
25. Liu, B.H.; Lin, H.; Chen, Y.F.; Liu, J.S.; Guo, C.; He, M.C.; Xu, X.D.; Shang, J.L.; Zheng, W.B. Deformation stability response of adjacent subway tunnels considering excavation and support of foundation pit. *Lithosphere* **2022**, *2022*, 7227330. [CrossRef]
26. Zhang, Y.; Yin, Z.Z.; Xu, Y.F. Analysis of surface deformation caused by shield tunneling. *Chin. J. Rock. Mech. Eng.* **2002**, *1*, 388–392. (In Chinese)
27. Zhang, Z.G.; Huang, M.S. Geotechnical influence on existing subway tunnels induced by multiline tunneling in Shanghai soft soil. *Comput. Geotech.* **2014**, *56*, 121–132. [CrossRef]
28. Sigl, O.; Atzl, G. Design of bored tunnel linings for Singapore MRT North East Line C706. *Tunn. Undergr. Space Technol.* **1999**, *14*, 481–490. [CrossRef]
29. Wang, Z.C.; Wang, H.T.; Zhu, X.G.; Zhao, D.S. Analysis of stratum deformation rules induced by the construction of double-tube parallel shield tunnels for Metro. *China Railw. Sci.* **2013**, *34*, 53–58. (In Chinese)
30. Fu, H.L.; Li, J.; Wang, H.T.; Zhang, J.B.; Huang, Z. Research on the ground settlement prediction in shallow tunnel under unsymmetrical pressure based on stochastic medium theory. *J. Railw. Eng. Soc.* **2017**, *34*, 70–76. (In Chinese)
31. Afifipour, M.; Sharifzadeh, M.; Shahriar, K.; Jamshidi, H. Interaction of twin tunnels and shallow foundation at Zand underpass, Shiraz metro, Iran. *Tunn. Undergr. Space Technol.* **2011**, *26*, 356–363. [CrossRef]